

LETTER TO THE EDITOR

Herschel observations in the ultracompact H II region Mon R2★

Water in dense Photon-dominated regions (PDRs)

A. Fuente¹, O. Berné², J. Cernicharo³, J.R. Rizzo³, M. González-García⁴, J.R. Goicoechea³, P. Pilleri^{5,6}, V. Ossenkopf^{7,8}, M. Gerin⁹, R. Güsten¹⁰, M. Akyilmaz⁷, A.O. Benz¹¹, F. Boulanger¹², S. Bruderer¹¹, C. Dedes¹¹, K. France¹³, S. García-Burillo¹⁴, A. Harris¹⁵, C. Joblin^{5,6}, T. Klein¹⁰, C. Kramer⁴, F. Le Petit¹⁶, S.D. Lord¹⁷, P.G. Martin¹³, J. Martín-Pintado³, B. Mookerjee¹⁸, D.A. Neufeld¹⁹, Y. Okada⁷, J. Pety²⁰, T.G. Phillips²¹, M. Röllig⁷, R. Simon⁷, J. Stutzki⁷, F. van der Tak^{8,22}, D. Teyssier²³, A. Usero¹⁴, H. Yorke²⁴, K. Schuster²⁰, M. Melchior²⁵, A. Lorenzani²⁶, R. Szczerba²⁷, M. Fich²⁸, C. McCoey^{28,29}, J. Pearson²⁴, P. Dieleman³⁰

(Affiliations can be found after the references)

Preprint online version: August 12, 2013

ABSTRACT

Context. Mon R2, at a distance of 830 pc, is the only ultracompact H II region (UC H II) where the photon-dominated region (PDR) between the ionized gas and the molecular cloud can be resolved with *Herschel*. Therefore, it is an excellent laboratory to study the chemistry in extreme PDRs ($G_0 > 10^5$ in units of Habing field, $n > 10^6$ cm⁻³).

Aims. Our ultimate goal is to probe the physical and chemical conditions in the PDR around the UC H II Mon R2.

Methods. HIFI observations of the abundant compounds ¹³CO, C¹⁸O, o-H₂¹⁸O, HCO⁺, CS, CH, and NH have been used to derive the physical and chemical conditions in the PDR, in particular the water abundance. The modeling of the lines has been done with the Meudon PDR code and the non-local radiative transfer model described by Cernicharo et al. (2006).

Results. The ¹³CO, C¹⁸O, o-H₂¹⁸O, HCO⁺ and CS observations are well described assuming that the emission is coming from a dense ($n = 5 \times 10^6$ cm⁻³, $N(\text{H}_2) > 10^{22}$ cm⁻²) layer of molecular gas around the H II region. Based on our o-H₂¹⁸O observations, we estimate an o-H₂O abundance of $\approx 2 \times 10^{-8}$. This is the average ortho-water abundance in the PDR. Additional H₂¹⁸O and/or water lines are required to derive the water abundance profile. A lower density envelope ($n \sim 10^5$ cm⁻³, $N(\text{H}_2) = 2.5 \times 10^{22}$ cm⁻²) is responsible for the absorption in the NH 1₁→0₂ line. The emission of the CH ground state triplet is coming from both regions with a complex and self-absorbed profile in the main component. The radiative transfer modeling shows that the ¹³CO and HCO⁺ line profiles are consistent with an expansion of the molecular gas with a velocity law, $v_e = 0.5 \times (r/R_{\text{out}})^{-1}$ km s⁻¹, although the expansion velocity is poorly constrained by the observations presented here.

Conclusions. We determine an ortho-water abundance of $\approx 2 \times 10^{-8}$ in Mon R2. Because shocks are unimportant in this region and our estimate is based on H₂¹⁸O observations that avoids opacity problems, this is probably the most accurate estimate of the water abundance in PDRs thus far.

Key words. ISM: structure – ISM: kinematics and dynamics – ISM: molecules – H II regions – Submillimeter

1. Introduction

Ultracompact (UC) H II regions constitute one of the earliest phases in the formation of a massive star and are characterized by extreme physical and chemical conditions ($G_0 > 10^5$ in units of Habing field and $n > 10^6$ cm⁻³). Their understanding is important for distinguishing the different processes in the massive star formation process and because they can be used as a template for other extreme photon-dominated regions (PDRs) such as the surface layers of circumstellar disks and/or the nuclei of starburst galaxies. The UC H II Mon R2 is the only one that can be resolved with *Herschel*.

Mon R2 is a nearby ($d = 830$ pc; Herbst & Racine 1976) complex star forming region. It hosts a UC H II region near its center, powered by the infrared source Mon R2 IRS1 (Wood & Churchwell 1989). The molecular content of this region has been the subject of several observational studies. The huge CO bipolar outflow (Meyers-Rice & Lada 1991), $\sim 15'$ long (≈ 3.6 pc) is a relic of the formation of the B0V star associ-

ated to IRS1 (Massi, Felli, & Simon 1985; Henning, Chini, & Pfau 1992) and strong shocks are currently not at work in this region (Berné et al. 2009). Previous molecular observations (Giannakopoulou et al. 1997; Tafalla et al. 1997; Choi et al. 2000; Rizzo et al. 2003, 2005) showed that the UC H II region is located inside a cavity and bound by a dense molecular ridge. The peak of this molecular ridge (hereafter, MP) is located at an offset (+10", -10") relative to the peak of the ionized gas (hereafter, IF). The molecular hydrogen column density toward the MP is $2 - 6 \times 10^{22}$ cm⁻². The detection of the reactive ions CO⁺ and HOC⁺ showed a dense photon-dominated region (PDR) surrounding the UC H II region (Rizzo et al. 2003, 2005). Recent Spitzer observations probed the thin molecular gas layer ($n = 4 \times 10^5$ cm⁻³, $N(\text{H}_2) = 1 \times 10^{21}$ cm⁻²) with $T_k = 574 (\pm 20)$ K in between the ionized gas and the dense molecular gas traced by previous millimeter observations (Berné et al. 2009). All these components are schematically shown in Fig. 1.

2. Observations

The observations were made with the HIFI instrument on-board *Herschel* (Pilbratt et al. 2010, de Graauw et al. 2010)

* *Herschel* is an ESA space observatory with science instruments provided by European-led Principal Investigator consortia and with important participation from NASA.

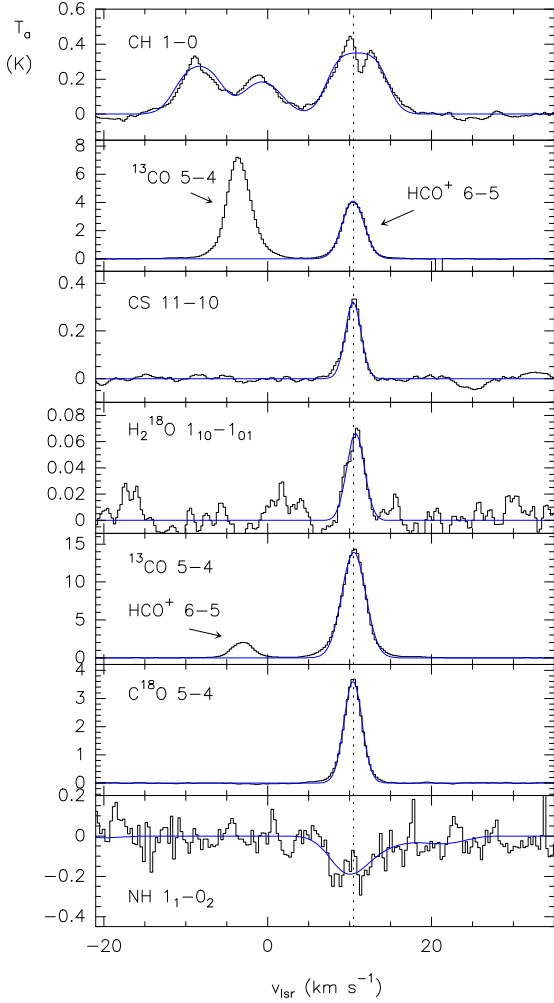


Fig. 2. HIFI spectra toward the MP in Mon R2. Note that the ^{13}CO 5 \rightarrow 4 and HCO^+ 6 \rightarrow 5 lines appear close in velocity. This is an artifact of the DSB observations. The HCO^+ 6-5 line is observed in the LSB and the ^{13}CO 5 \rightarrow 4 line, in the USB. The dashed line indicates $v_{\text{LSR}}=10.5 \text{ km s}^{-1}$.

during the Priority Science Phase 2 in the frequency switch (FSW) observing mode with a reference position at the offset (+10',0). Two receiver settings were observed, one in Band 1a with the WBS centered at 536.066GHz (LSB) and the other in Band 4a with the WBS centered at 971.800 GHz (LSB). These settings were observed toward both positions, IF [RA=06h07m46.2s, DEC=-06°23'08.3" (J2000)] and MP [RA=06h07m46.87s, DEC=-06°23'18.3" (J2000)]. In this letter we present the observations toward the MP because the study of the spatial distribution of the molecular tracers is postponed for a forthcoming paper. The data were reduced using HIPE 3.0 pipeline. The adopted intensity scale was antenna temperature. In addition to *Herschel* data, we used the HCO^+ (1 \rightarrow 0), HCO^+ (3 \rightarrow 2), CS (2 \rightarrow 1), ^{13}CO (1 \rightarrow 0), ^{13}CO (2 \rightarrow 1), C^{18}O (1 \rightarrow 0) and C^{18}O (2 \rightarrow 1) observed with the IRAM 30m telescope.

3. Results

We detected the CH 1 \rightarrow 0, HCO^+ 6 \rightarrow 5, CS 11 \rightarrow 10, o- H_2^{18}O 1 $_{10}\rightarrow$ 1 $_{01}$, ^{13}CO 5 \rightarrow 4, C^{18}O 5 \rightarrow 4, and NH 1 $_{1}\rightarrow$ 0 $_{2}$ lines in the MP (see Fig. 2). We stress that this is the first detection of the rarer water isotopologue o- H_2^{18}O toward a spatially resolved

Table 1. Summary of HIFI observations

Line	Freq. (GHz)	$T_a \times \tau$ (K)	v_{LSR} (km s $^{-1}$)	Δv (km s $^{-1}$)	τ
CH	536.761	1.81(0.21)	10.9(0.1)	4.9(0.3)	3.6(0.6)
NH	974.478	-0.24(0.07)	9.9(0.4)	4.9(0.8)	0.1(0.7)
Line	Freq. (GHz)	Area (K \times km s $^{-1}$)	v_{LSR} (km s $^{-1}$)	Δv_{LSR} (km s $^{-1}$)	T_{MB} (K)
HCO^+	535.061	19.4(4.0)	10.4(0.3)	3.2(0.8)	5.7
CS	538.688	1.09(0.04)	10.5(0.1)	2.2(0.1)	0.4
o- H_2^{18}O	547.676	0.22(0.03)	10.7(0.1)	2.4(0.3)	0.08
^{13}CO	550.926	51.1(2.0)	10.6(0.1)	3.4(0.2)	14.0
C^{18}O	548.830	14.0(0.4)	10.5(0.1)	2.6(0.1)	5.0

PDR. All the lines except NH 1 \rightarrow 0 $_{2}$ were detected in emission. Gaussian fits are shown in Table 1 and Fig. 2. We fitted the three components of the CH 1 \rightarrow 0 line assuming the same excitation temperature and estimated that the opacity of the main component is >3 . In this case, the central velocity is not well determined because of the self-absorption and the flattened profiles produced by the large opacities. The NH 1 \rightarrow 0 $_{2}$ line was tentatively detected ($\sim 3\sigma$) in absorption. This line is composed of 10 components and we fitted all of them assuming the same excitation temperature. Our fit shows that the NH line is optically thin. Because the individual components are not resolved with a linewidth of $\sim 4 \text{ km/s}$, the individual line parameters are uncertain. This detection needs to be confirmed.

3.1. Line profiles

Different velocity components can be distinguished in this region. The ambient cloud is centered at $v_{\text{LSR}}=10.5 \pm 1 \text{ km s}^{-1}$. A large scale molecular outflow is associated with IRS 1 (Meyers-Rice & Lada, C.J. 1991; Tafalla et al. 1997). The wings observed in the emission profiles of the HCO^+ 1 \rightarrow 0 and 3 \rightarrow 2 lines and in the ^{13}CO 2 \rightarrow 1 line (velocity ranges [0,6] km s $^{-1}$ and [4,14] km s $^{-1}$) are associated with the molecular outflow. The HCO^+ 6 \rightarrow 5, ^{13}CO 5 \rightarrow 4 and C^{18}O 5 \rightarrow 4 lines are centered at a velocity of $\sim 10.4 \text{ km s}^{-1}$. In Fig. 3 we compare the HIFI lines with the low rotational lines of the same species observed with the IRAM 30m telescope. The angular resolution of the IRAM data was degraded to match those of *Herschel*. The line profiles of the low rotational lines of HCO^+ and ^{13}CO are self-absorbed at red-shifted velocities. For C^{18}O , there is a perfect match between the profiles of the the J=5 \rightarrow 4 and J=2 \rightarrow 1 lines. The profiles of the CS J=2 \rightarrow 1 and J=11 \rightarrow 10 lines also match perfectly.

The HCO^+ 6 \rightarrow 5, CS 11 \rightarrow 10, ^{13}CO 5 \rightarrow 4 and C^{18}O 5 \rightarrow 4 lines have characteristic linewidths of 2–3 km s $^{-1}$. The largest linewidths observed in the NH 1 \rightarrow 0 $_{2}$ and CH lines ($\sim 5 \text{ km s}^{-1}$) indicate that these lines are tracing a different, probably more diffuse component. As argued in Sect 4.1, the NH absorption is very likely caused by the cold and lower density envelope surrounding the UC HII region. The CH 1 \rightarrow 0 line is seen in absorption and emission suggesting that CH is present in the low density envelope and the dense PDR.

3.2. Molecular column densities

In Table 2 we present the estimated molecular column densities. We used the rotational diagram technique to estimate the rotation temperature and the column density of the CO isotopologues and CS. This technique gives an average rotation temperature and total column density providing that the emission is optically thin. For optically thick lines, we obtained a lower limit to the true

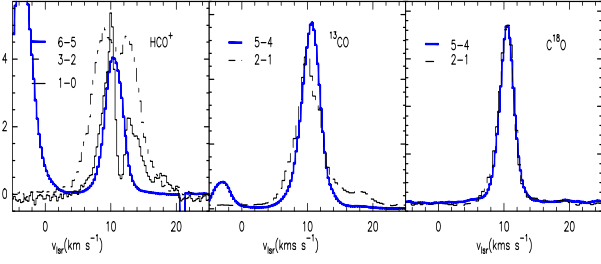


Fig. 3. Comparison of the profiles of the HIFI and IRAM 30m spectra toward the MP in Mon R2. The high angular resolution 30m spectra were degraded to match the angular resolution of *Herschel* data (40"). The ^{13}CO 1 \rightarrow 0 and C^{18}O 1 \rightarrow 0 lines are not included because we observed them with a poor spectral resolution (1.5 MHz \sim 7 km s $^{-1}$).

column density and rotation temperature (this is very likely the case for ^{13}CO). For CH and NH we assumed a reasonable value of the rotation temperature. Previous molecular observations at millimeter wavelengths showed the existence of gas with densities up to $n=4\times 10^6$ cm $^{-3}$ and $T_k\approx 50$ K in the molecular ridge (Choi et al. 2000; Rizzo et al. 2003, 2005). Berné et al. (2009) derived a density, $n=4\times 10^5$ cm $^{-3}$ and a gas kinetic temperature of ~ 570 K for a thin gas layer around the H II region on basis of the H_2 rotational lines. These two n-T pairs of values can produce the rotation temperatures derived from our observations. However, the gas layer at 570 K cannot account for the observed line intensities. For instance, assuming a standard C^{18}O abundance of 2×10^{-7} , this hot layer will produce a C^{18}O 5 \rightarrow 4 line intensity of $T_b\sim 0.09$ K, i.e. 2% of the observed value. Therefore, the emission of the observed lines is mainly coming from the dense ($n=4\times 10^6$ cm $^{-3}$) molecular ridge.

We detected the o- H_2^{18}O 1 $_{10}\rightarrow$ 1 $_{01}$ line in the MP. Using the non-local radiative transfer code of Cernicharo et al. (2006) and assuming the densities and temperatures prevailing in the dense molecular ridge ($T_k=50$ K, $n(\text{H}_2)=4\times 10^6$ cm $^{-3}$), we obtained an excitation temperature for the ground state transition of o- H_2^{18}O of ~ 8.5 K. With this low excitation temperature, we need $N(\text{o-}\text{H}_2^{18}\text{O})=2.7\times 10^{12}$ cm $^{-2}$ to fit our observations. Assuming a $^{18}\text{O}/^{16}\text{O}$ ratio of ~ 500 , this implies an ortho-water abundance of $\sim 2\times 10^{-8}$. The excitation temperature is not very sensitive to the gas kinetic temperature. To assume a gas kinetic temperature as high as 500 K would increase the excitation temperature by a factor of 2, and decrease the estimated o- H_2^{18}O column density by a factor of 10. To assume a lower hydrogen density would be more critical, because the excitation temperature would drop to very low values (<6 K), and the line would become very weak and optically thick which would prevent any good estimate of the o- H_2^{18}O column density. The water abundance estimated in Mon R2 is similar to that obtained toward the Orion Bar by Olofsson et al. (2003) using ODIN observations. In that case, the spatial resolution of the ODIN observations did not allow the authors to resolve the dense PDR. Moreover, their estimate was based on observations of the ground state transition of the main water isotopologue, which is optically thick. The agreement between the two measurements could therefore be fortuitous. Recent SPIRE observations of the Orion Bar have provided an upper limit to the water abundance of a few 10^{-7} (Habart et al. 2010).

To interpret the observed NH 1 $_1$ -0 $_2$ line absorption, a knowledge of the continuum level is needed. Unfortunately, the line was observed in FSW mode, which removes the continuum.

Table 2. Molecular column densities*

Mol	T_{rot} (K)	Observed (cm $^{-2}$)	PDR Model (cm $^{-2}$)
^{13}CO	27	$4.7 \cdot 10^{16}$	$3.5 \cdot 10^{16b}$
C^{18}O	34	$6.9 \cdot 10^{15}$	$3.5 \cdot 10^{15b}$
H^{13}CO^+	20 ^c	$1.7 \cdot 10^{12c}$	$9.3 \cdot 10^{11b}$
CS	25	$6.3 \cdot 10^{13}$	$6.7 \cdot 10^{13}$
o- H_2^{18}O	8.5 ^a	$2.7 \cdot 10^{12}$	$2.9 \cdot 10^{12b,d}$
CH	19 ^a	$5.6 \cdot 10^{13}$	$3.3 \cdot 10^{14}$
NH	10-20 ^a	$1.5 \cdot 10^{13}$	$5.1 \cdot 10^{11}$

* The rotational diagrams used the 30m and HIFI lines.

^a Assumed rotational temperature.

^b Assuming $^{12}\text{C}/^{13}\text{C}=50$ and $^{16}\text{O}/^{18}\text{O}=500$

^c From Rizzo et al. (2005)

^d Assuming an ortho-to-para ratio of 3.

Hence, the continuum level had to be estimated from previous measurements. In particular, Dotson et al. (2010) measured an intensity of 280 Jy/beam using the CSO telescope (beam=20") at 350 μm (=857 GHz). Assuming a spectral index β of ~ 3 , we estimate a continuum flux of 411 Jy at 974 GHz. This value corresponds to a brightness temperature of 0.8 K in the HIFI beam. Taking into account the uncertainty in β and the different beams of *Herschel* and CSO, we estimate that the accuracy of the continuum intensity at 974 GHz is about a factor of 2. Assuming $T_{ex}=10$ K, and an intrinsic linewidth of 4 km s $^{-1}$, the line opacity inferred from the observed absorption feature implies a NH column density of $(1-5)\times 10^{13}$ cm $^{-2}$ (a factor ~ 1.5 higher if $T_{ex}=20$ K). Taking $\sim 5\times 10^{22}$ cm $^{-2}$ as an upper limit for $N(\text{H}_2)$ (the NH absorption likely arises in an external layer of more diffuse gas), the NH abundance would be greater than $(1.0-0.2)\times 10^{-9}$. These abundances are comparable to the NH abundance first inferred by ISO toward Sgr B2 (Cernicharo et al. 2000, Goicoechea et al. 2004).

4. Discussion

4.1. Chemical model

We explored the possibility of explaining the molecular abundances observed in Mon R2 in terms of PDR chemistry. To do this, we used the updated version of the Meudon PDR code (Le Petit et al. 2006, Goicoechea & Le Bourlot 2007). As input parameters we used a plane-parallel slab with a thickness of 10 mag and $n=4\times 10^6$ cm $^{-3}$, which is illuminated from the left side with a field of $G_0=5\times 10^5$ and from the right side with the standard interstellar UV field ($G_0=1$). Elemental abundances were: He (0.1), O (3.19×10^{-4}), N (7.5×10^{-5}), C (1.32×10^{-4}), S (1.86×10^{-5}), Fe (1.5×10^{-8}). The model does not include isotopic fractionation, we estimated the abundances of the isotopologues assuming $^{12}\text{CO}/^{13}\text{CO}=50$ and $^{16}\text{O}/^{18}\text{O}=500$. The obtained column densities are shown in Table 2 and the abundance profiles are plotted in Fig. 4. We got an excellent agreement between observations and model predictions for the CO isotopologues, HCO^+ , H_2O , and CS. The model successfully predicts the observed average water abundance. The water abundance is far from uniform across the PDR, with a peak of $\sim 10^{-6}$ at an extinction of ~ 1 mag and a minimum value $<10^{-10}$ (see Fig. 4). The observation of high excitation lines of water will allow us to derive the water abundance profile and further constrain the chemical modeling. The model falls short by more than one order of magnitude however to predict the NH column density. The

NH abundance is $<10^{-9}$ all across the PDR (see Fig. 4). As argued below, this is very likely due to the main contribution to the observed NH line coming from the low density envelope that is protected from the UV radiation. We ran the code for a low density ($n \approx 4 \times 10^4 \text{ cm}^{-3}$) plane-parallel layer of 50 mag illuminated with $G_0=1$ and obtain a NH column density of $\sim 3 \times 10^{13} \text{ cm}^{-2}$ in better agreement with the observations. This low density envelope would also contribute to the CH ground state line since the CH column density should be \sim a few 10^{14} cm^{-2} . For this reason, we have a very complex CH profile, with the line optically thick and self-absorption in the main component. However, the contribution of the low density envelope to the other observed HIFI lines would be negligible because of the low density and low gas kinetic temperature. For instance, the intensity of the ^{13}CO $5 \rightarrow 4$ line would be $\sim 0.1 \text{ K}$.

4.2. Kinematics of the region

The systematic change in the line profiles of the rotational lines of HCO^+ and ^{13}CO can be understood in terms of the velocity structure of the molecular core. Although the complete modeling of the source is beyond the scope of this paper, (most of the HIFI data are still to come), we made a preliminary model to gain insights into the kinematics of this source. The UC H II region is expected to expand because of the different pressure of the ionized and molecular gas (Jaffe et al. 2003; Rizzo et al. 2005). We modeled the HCO^+ and ^{13}CO lines using the non-local radiative transfer code of Cernicharo et al. (2006). In the model, we adopted the physical structure derived in Sect. 4.1 (a spherical envelope with inner radius $R_{in}=0.08 \text{ pc}$, an innermost layer with $T_k=50 \text{ K}$, $n=4 \times 10^6 \text{ cm}^{-3}$ and a radial thickness of 0.0006 pc , and an external envelope with the temperature decreasing as $T \propto R^{-0.5}$, a constant density of $n=1 \times 10^5 \text{ cm}^{-3}$ and a thickness of 0.16 pc). For the dust temperature and opacity, we adopted the values derived by Thronson et al. (1980). As a first approximation we assumed constant ^{13}CO and HCO^+ abundances of 2×10^{-6} and 10^{-9} respectively and only varied the velocity law. We were able to reproduce the line intensities and the trend observed in the line profiles assuming an expansion velocity law $v_e = 0.5 \times (R/R_{out})^{-1} \text{ km s}^{-1}$ ($R_{out}=0.24 \text{ pc}$) and a turbulent velocity of 2 km s^{-1} (see Fig. 5). Because of the hole in the molecular core, the maximum expansion velocity is 1.5 km s^{-1} , which is similar to the turbulent velocity. For this reason, the back and front parts of the envelope are radiatively coupled producing the self-absorbed profiles at red-shifted velocities. The shapes of the line profiles are dominated by the turbulent velocity with little effect of the small expansion velocity, which is poorly constrained.

5. Conclusions

We present the first HIFI observations toward the UC H II region Mon R2. Detections of the ^{13}CO $5 \rightarrow 4$, C^{18}O $5 \rightarrow 4$, $\text{o-H}_2^{18}\text{O}$ $1_{10} \rightarrow 1_{01}$, HCO^+ $6 \rightarrow 5$, CS $11 \rightarrow 10$, NH 1_1-0_2 , and CH $1 \rightarrow 0$ lines are reported. The emission/absorption of all these molecules is well explained assuming the the molecular core is composed of a dense ($n=5 \times 10^6 \text{ cm}^{-3}$) PDR layer of gas surrounded by a lower density UV protected envelope. The modeling of the ^{13}CO and HCO^+ line profiles is consistent with the molecular gas being expanding with an expansion velocity law, $v_e = 0.5 \times (r/R_{out})^{-1} \text{ km s}^{-1}$. Based on our $\text{o-H}_2^{18}\text{O}$ $1_{10} \rightarrow 1_{01}$ observations, we estimate an ortho-water abundance of $\sim 2 \times 10^{-8}$. Because shocks are unimportant in this region and our estimate

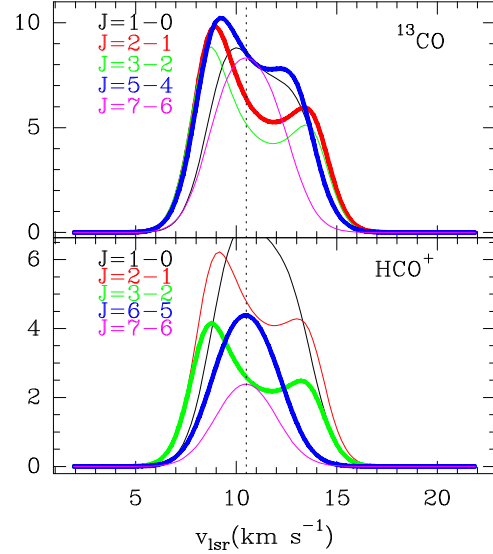


Fig. 5. Predicted line profiles for the ^{13}CO and HCO^+ rotational lines using the model described in Sect 4.2.

is based on the rarer isotopologue observations that avoids opacity problems, this water abundance estimate is probably the most accurate in PDRs thus far.

Acknowledgements. HIFI has been designed and built by a consortium of institutes and university departments from across Europe, Canada and the United States under the leadership of SRON Netherlands Institute for Space Research, Groningen, The Netherlands and with major contributions from Germany, France and the US. Consortium members are: Canada: CSA, U.Waterloo; France: CESR, LAB, LERMA, IRAM; Germany: KOSMA, MPIfR, MPS; Ireland, NUI Maynooth; Italy: ASI, IFSI-INAF, Osservatorio Astrofisico di Arcetri-INAF; Netherlands: SRON, TUD; Poland: CAMK, CBK; Spain: Observatorio Astronómico Nacional (IGN), Centro de Astrobiología (CSIC-INTA). Sweden: Chalmers University of Technology - MC2, RSS & GARD; Onsala Space Observatory; Swedish National Space Board, Stockholm University - Stockholm Observatory; Switzerland: ETH Zurich, FHNW; USA: Caltech, JPL, NHSC. This paper was partially supported by Spanish MICINN under project AYA2009-07304 and within the program CONSOLIDER INGENIO 2010, under grant Molecular Astrophysics: The Herschel and ALMA Era ASTROMOL (ref.: CSD2009-00038).

References

- Berné, O., Fuente, A., Goicoechea, J. R., Pilleri, P., González-García, M., & Joblin, C. 2009, *ApJL*, 706, L160
Cernicharo, J., Goicoechea, J. R., & Caux, E. 2000, *ApJL*, 534, L199
Cernicharo, J., Goicoechea, J. R., Pardo, J. R., & Asensio-Ramos, A. 2006, *ApJ*, 642, 940
Choi, M., Evans, N. J., II, Tafalla, M., & Bachiller, R. 2000, *ApJ*, 538, 738
de Graauw T. et al., 2010, this volume.
Dotson, J. L., Vaillancourt, J. E., Kirby, L., Dowell, C. D., Hildebrand, R. H., & Davidson, J. A. 2010, *ApJS*, 186, 406
Giannakopoulou, J., Mitchell, G. F., Hasegawa, T. I., Matthews, H. E., & Maillard, J.-P. 1997, *ApJ*, 487, 346
Goicoechea, J. R., Rodríguez-Fernández, N. J., & Cernicharo, J. 2004, *ApJ*, 600, 214
Goicoechea, J. R., & Le Bourlot, J. 2007, *A&A*, 467, 1
Habart, E. et al., 2010, *A&A Herschel* Special Issue
Henning, T., Chini, R., & Pfau, W. 1992, *A&A*, 263, 285
Herbst, W., & Racine, R. 1976, *AJ*, 81, 840
Jaffe, D. T., Zhu, Q., Lacy, J. H., & Richter, M. 2003, *ApJ*, 596, 1053
Le Petit, F., Nehmé, C., Le Bourlot, J., & Roueff, E. 2006, *ApJS*, 164, 506
Massi, M., Felli, M., & Simon, M. 1985, *A&A*, 152, 387
Meyers-Rice, B. A., & Lada, C. J. 1991, *ApJ*, 368, 445
Olofsson, A. O. H., et al. 2003, *A&A*, 402, L47
Pilbratt, G., et al. 2010, this volume

- Rizzo, J. R., Fuente, A., Rodríguez-Franco, A., & García-Burillo, S. 2003, *ApJL*, 597, L153
Rizzo, J. R., Fuente, A., & García-Burillo, S. 2005, *ApJ*, 634, 1133
Tafalla, M., Bachiller, R., Wright, M. C. H., & Welch, W. J. 1997, *ApJ*, 474, 329
Thronson, H. A., Jr., Gatley, I., Harvey, P. M., Sellgren, K., & Werner, M. W. 1980, *ApJ*, 237, 66
Wood, D. O. S., & Churchwell, E. 1989, *ApJS*, 69, 831

-
- ¹ Observatorio Astronómico Nacional (OAN), Apdo. 112, 28803 Alcalá de Henares (Madrid), Spain
² Leiden Observatory, Universiteit Leiden, P.O. Box 9513, NL-2300 RA Leiden, The Netherlands
³ Centro de Astrobiología, CSIC-INTA, 28850, Madrid, Spain
⁴ Instituto de Radio Astronomía Milimétrica (IRAM), Avenida Divina Pastora 7, Local 20, 18012 Granada, Spain
⁵ Université de Toulouse, UPS, CESR, 9 avenue du colonel Roche, 31062 Toulouse cedex 4, France
⁶ CNRS, UMR 5187, 31028 Toulouse, France
⁷ I. Physikalisches Institut der Universität zu Köln, Zùlpicher Straße 77, 50937 Köln, Germany
⁸ SRON Netherlands Institute for Space Research, P.O. Box 800, 9700 AV Groningen, Netherlands
⁹ LERMA, Observatoire de Paris, 61 Av. de l'Observatoire, 75014 Paris, France
¹⁰ Max-Planck-Institut für Radioastronomie, Auf dem Hügel 69, 53121, Bonn, Germany
¹¹ Institute for Astronomy, ETH Zürich, 8093 Zürich, Switzerland
¹² Institut d'Astrophysique Spatiale, Université Paris-Sud, Bât. 121, 91405 Orsay Cedex, France
¹³ Department of Astronomy and Astrophysics, University of Toronto, 60 St. George Street, Toronto, ON M5S 3H8, Canada
¹⁴ Observatorio Astronómico Nacional (OAN), Alfonso XII, 3, 28014 Madrid, Spain
¹⁵ Astronomy Department, University of Maryland, College Park, MD 20742, USA
¹⁶ Observatoire de Paris, LUTH and Université Denis Diderot, Place J. Janssen, 92190 Meudon, France
¹⁷ IPAC/Caltech, MS 100-22, Pasadena, CA 91125, USA
¹⁸ Tata Institute of Fundamental Research (TIFR), Homi Bhabha Road, Mumbai 400005, India
¹⁹ Department of Physics and Astronomy, Johns Hopkins University, 3400 North Charles Street, Baltimore, MD 21218, USA
²⁰ Institut de Radioastronomie Millimétrique, 300 Rue de la Piscine, 38406 Saint Martin d'Hères, France
²¹ California Institute of Technology, 320-47, Pasadena, CA 91125-4700, USA
²² Kapteyn Astronomical Institute, University of Groningen, PO box 800, 9700 AV Groningen, Netherlands
²³ European Space Astronomy Centre, Urb. Villafranca del Castillo, P.O. Box 50727, Madrid 28080, Spain
²⁴ Jet Propulsion Laboratory, 4800 Oak Grove Drive, Pasadena, CA 91109 U.S.A.
²⁵ Institut für 4D-Technologien, FHNW, 5210 Windisch, Switzerland
²⁶ Osservatorio Astrofisico di Arcetri-INAF- Largo E. Fermi 5 I-50100 Florence, Italy
²⁷ N. Copernicus Astronomical Center, Rabianska 8, 87-100, Torun, Poland
²⁸ Department of Physics and Astronomy, University of Waterloo, Waterloo, ON Canada N2L 3G1
²⁹ University of Western Ontario, Dept. of Physics & Astronomy, London, Ontario, Canada N6A 3K7
³⁰ SRON Netherlands Institute for Space Research, Landleven 12, 9747 AD Groningen

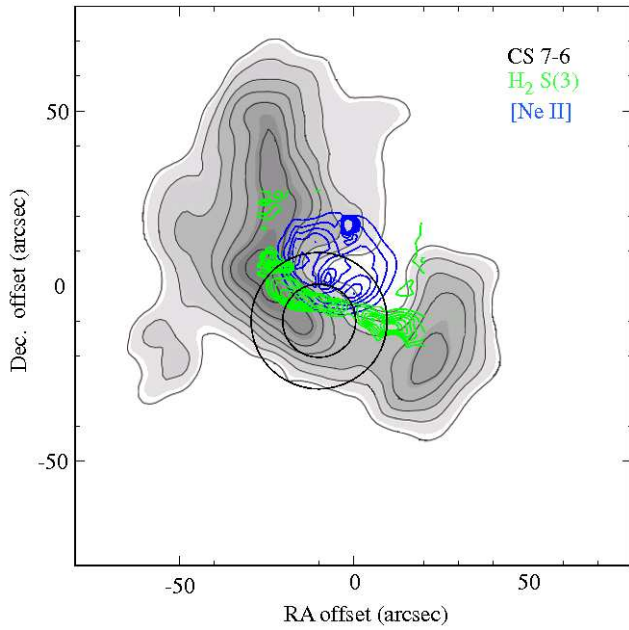


Fig. 1. Overview of the PDR associated with Mon R2. Gray scales represent the CS 7→6 line emission map from Choi et al. (2000). The blue contours represent the intensity of the [Ne II] line ($0.02\text{--}0.1 \text{ erg s}^{-1} \text{ cm}^{-2} \text{ sr}^{-1}$ in linear steps), and the green contours the intensity of the H_2 S(3) rotational line at $9.7 \mu\text{m}$ ($1.5\text{--}4.5 \times 10^4 \text{ erg s}^{-1} \text{ cm}^{-2} \text{ sr}^{-1}$ in linear steps). The circles indicate the *Herschel* beam in band 1a ($40''$) and band 4a ($21''$) centered on the molecular peak (MP).

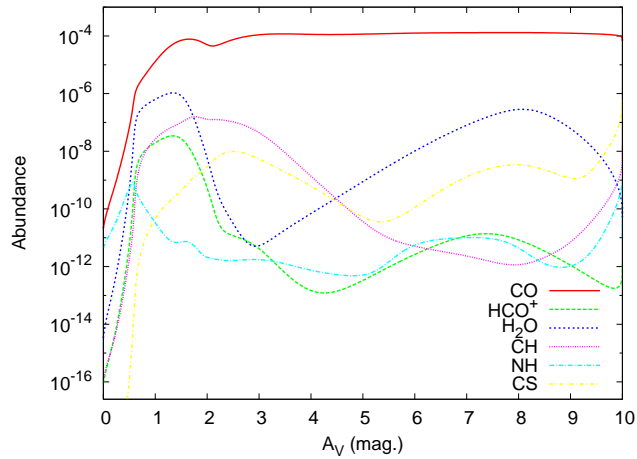


Fig. 4. Results of the chemical modeling of the dense PDR surrounding the UCHII region Mon R2